# Time-Varying Analysis of Vehicle-Bridge Interaction System for bridge health monitoring using Synchrosqueezing Transform


Mingzhe Gao, Xinqun Zhu, Jianchun Li
School of Civil and Environmental Engineering, University of Technology,
Sydney, NSW 2007, Australia
Email: Mingzhe.Gao@student.uts.edu.au, Xinqun.Zhu@uts.edu.au, Jianchun.Li@uts.edu.au



ABSTRACT: The passage of the vehicle over the bridge is a time-varying process. The bridge damage will cause a change in the time-varying characteristics of the vehicle-bridge interaction (VBI) system. This paper presents a synchrosqueenzing transform based method for extracting the time-varying characteristics from the dynamic response of the bridge subject to a moving vehicle. A numerical and experimental study has been conducted to show the performance of the proposed method. The bridge damage is simulated as a damage zone with three parameters representing the location, range and severity of the damage. The instantaneous frequency is obtained by the edge detection from the time-frequency representation of bridge dynamic response. The results show that the time-varying characteristics of the VBI system using the proposed method could be a good indicator of bridge damage.



KEY WORDS: Time-varying characteristics, Synchrosqueezing Transform, vehicle-bridge interaction.


## 1 INTRODUCTION

Structural Health Monitoring (SHM) represents a crucial technological advancement in maintaining bridge integrity by offering key insights into bridge health through vibration response monitoring. Recently, vehicle-bridge interaction (VBI) based bridge SHM attracts the interest of researchers and engineers [1]. Structural damage will cause the change in dynamic responses and the damage could be detected using the features from dynamic responses. The structural damage is normally a nonlinear phenomenon and time-varying characteristics from dynamic responses of the bridge under moving vehicles could be a good indicator of structural damage [2]. The passage of the vehicle over the bridge is a time-varying process. It is a big challenge to extract the time-varying characteristics of the VBI system for bridge SHM.

Time-frequency analysis techniques have been widely used in SHM. The short-time Fourier transform (STFT) and the continuous wavelet transform (CWT) are the most typical time frequency analysis. STFT has the fixed time-frequency localization and CWT has a varying time-frequency localization. Both STFT and CWT suffer from the finite localization and the reduced readability due to spectral smoothing and leakage [3]. A new signal processing technique known as Synchrosqueezing Transform (SST) has been used to enhance the resolution. Various SST algorithms have been developed, such as the STFT based SST [4] and the CWT based SST [5]. This paper is to extract the time-varying characteristics of the VBI system using these two algorithms.

Recently, time-frequency analysis techniques have been used to extract the time-varying characteristics of the VBI system. Li et al are the first to use the time-frequency analysis method to analyse the time-varying characteristics of the VBI system [6]. The synchroextrcting transform is used and that is based on the assumption of linear frequency modulation and constant amplitude signal. A modified S-transform method has been proposed to extract the fundamental frequency of the bridge from the bridge response [7]. The second-order SST is used to explore the time-varying nature of frequencies in the VBI system [8]. As the above, the time-varying characteristics of the VBI system with the damage has not been studied.

The paper presents a new SST based method for extracting the time-varying characteristics of the VBI system for bridge SHM. Numerical and experimental studies have been used to show the performance of the proposed method. The bridge damage is simulated as a damage zone with three parameters. The results show that the time-varying characteristics of the VBI system is an effective damage indicator.

## 2 VEHICLE-BRIDGE INTERACTION SYSTEMS

### 2.1 *Vehicle-bridge interaction modeling*

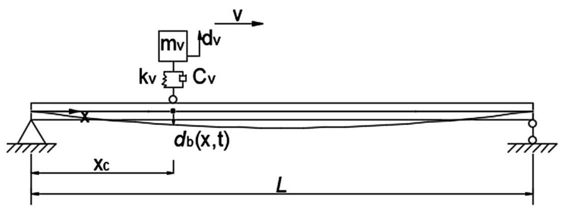


Figure 1. Vehicle-bridge interaction model.

As shown in Figure 1, the bridge-vehicle system is represented as a continuous uniform beam subjected to a moving vehicle. The vehicle is assumed to be travelling collectively along the longitudinal direction of the beam from left to right at a constant speed v. The bridge is modelled as a simply-supported Euler-Bernoulli beam. The bridge is modelled using the finite element model. The equations of motion for the bridge and vehicle model can be expressed as follows [1]

$$m_v\ddot{d}_v(t) + c_v\dot{d}_v(t) + k_v d_v(t) = P_{vint}(t) \quad (1)$$

$$\mathbf{M}_b\ddot{\mathbf{d}}_b(t) + \mathbf{C}_b\dot{\mathbf{d}}_b(t) + \mathbf{K}_b\mathbf{d}_b(t) = \mathbf{H}_c(t)P_{\mathrm{bint}}(t) \quad (2)$$

where $\ddot{d}_v, \dot{d}_v, d_v$ are the vertical acceleration, velocity and displacement of the vehicle respectively. $\ddot{\mathbf{d}}_b, \dot{\boldsymbol{d}}_b, \boldsymbol{d}_b$ denotes the vertical acceleration, velocity and displacement responses of the bridge, respectively. $\mathbf{M}_b$, $\mathbf{C}_b$, $\mathbf{K}_b$ are the mass, damping and stiffness matrices of the bridge, respectively. $P_{vint}(t) = k_v d_{cp}(t) + c_v\dot{d}_{cp}(t)$ is the force for the bridge to the vehicle system. $d_{cp}(t) = d_b(x(t), t) + r(x(t))$ is the contact displacement between the vehicle and bridge at the location $x(t)$ . $r(x)$ is the road surface roughness. $P_{\text{bint}}(t) = m_v g - P_{vint}$ is the interacting force for the vehicle to the bridge. $\mathbf{H}_c(t) = \{\mathbf{0},\ \mathbf{0},\ \ldots,\ \boldsymbol{H}_i(t), \ldots,\ \mathbf{0}\}^T$ is a function of time. $\boldsymbol{H}_i(t)$ is the vector of the shape function in the $i^{th}$ element on which the moving vehicle is located at time instant *t* as,

$$\boldsymbol{H}_i(t) = \{1 - 3\xi(t)^2 + 2\xi(t), (\xi(t) - 2\xi(t)^2 + \xi(t)^3)l_e, 3\xi(t)^2 - 2\xi(t)^3, (-\xi(t)^2 + \xi(t)^3)l_e\}^T \tag{3}$$

where $\xi(t) = (x(t) - (\mathrm{i} - 1)l_e)/l_e$. (i-1)$l_e \le x(t) \le il_e$. $l_e$ is the length of the element.

### 2.2 The damage model

Considering a reinforced concrete beam, the damage is simulated as a reduction in the flexural rigidity as [9]:

$$EI(x) = E_0 I\left(1 - \alpha\cos^2\left(\frac{\pi}{2}\left(\frac{|x-l_c|}{\beta L/2}\right)^m\right)\right) \tag{4}$$

$$(l_c - \beta L/2 < x < l_c + \beta L/2)$$

where $l_c$ is the central location of the damage zone measured from the left end support. $\beta$ is a dimensionless parameter to define the length of the damaged zone, which has a range of 0.0 to 1.0. $\alpha$ is a dimensionless parameter to describe the severity of the damage, which is between 0.0 to 1.0. There is no damage if $\alpha$ = 0.0. The flexural regidity varies from the damage zone's centre to its two extremes, and this variation is described by parameter $m$. $E_0$ is the Young's modulus of the intact beam. According to Equation (4), the equivalent damage element stiffness matrix can be obtained [9].

## 3 TIME-VARYING ANALYSIS USING SST

### 3.1 Short Fourier transform (STFT) based SST

The function of STFT g∈L2 (R) is defined in terms of the real and even windows.

$$G(t,\omega) = \int_{-\infty}^{+\infty} g(u-t)s(u)e^{-i\omega(u-t)}du \tag{5}$$

where $g(u)$ supports in $[-\Delta_t, \Delta_t]$, the monocomponent signal model is

$$s(t) = A(t)e^{i\varphi(t)} \tag{6}$$

where $\exists\varepsilon$ is small, therefore$|A'(t)| \le \varepsilon$ and $|\varphi''(t)| \le \varepsilon\forall t$.

The signal can be defined as:

$$s(u) = A(t)e^{i(\varphi(t)+\varphi'(t)(u-t))} \tag{7}$$

Therefore, the STFT function can be defined as:

$$\begin{aligned} G(S,\omega) &= \int_{-\infty}^{+\infty} g(u-t)A(t)e^{i(\varphi(t)+\varphi'(t)(u-t))}e^{-i\omega(u-t)}du \\ &= A(t)e^{i\varphi(t)}\int_{-\infty}^{+\infty} g(u-t)e^{i(\varphi'(t)(u-t))-i\omega(u-t)}d(u-t) \\ &= A(t)e^{i\varphi(t)}\hat{g}(\omega - \varphi'(t)) \end{aligned} \tag{8}$$

where for any $(t,\omega)$ , $G(t,\omega) \ne 0$, therefore, a two-dimension instantaneous frequency (IF) $\hat{\omega}(t,\omega)$ can be defined as,

$$\hat{\omega}(t,\omega) = \frac{\partial_t G(t,\omega)}{iG(t,\omega)} \tag{9}$$

It has been demonstrated that by setting $\tilde{\varepsilon} = \varepsilon^{1/3}$ and assuming that is sufficiently small, we have the approximation, for $G(t,\omega)\ |\ge \tilde{\varepsilon}$.

$$|\hat{\omega}(t,\omega) - \varphi'(t)| \le \tilde{\varepsilon} \tag{10}$$

To collect the time-frequency coefficients, the SST uses a frequency-reassignment operator, which is represented as [4]

$$Ts(t,\eta) = \int_{-\infty}^{+\infty} G(t,\omega)\delta(\eta - \hat{\omega}(t,\omega))d\omega \tag{11}$$

The time-frequency coefficient for the IF trajectory is extracted in this post-processing approach, and the rest of the time-frequency coefficients are ignored. To reduce the noise influence on the time-frequency result, the greatest time-frequency coefficient is employed to construct the unique time-frequency representation in this study.

### 3.2 Continuous wavelet transform based SST

The continuous wavelet transform (CWT) of a signal $f(t) \in L^2(R)$ is defined as

$$W_f(a,b) = \frac{1}{\sqrt{a}}\int_{-\infty}^{+\infty} f(t)\psi^*\left(\frac{t-b}{a}\right)dt \tag{12}$$

where $\psi^*$ relates to the wavelet's complex conjugate. For any $(a,b)$ , $W(t,\omega) \ne 0$. A 2D IF $\omega_x(a,b)$ can be defined as,

$$\omega_x(a,b) = \frac{\frac{\partial}{\partial b}W_x(a,b)}{2\pi i W_x(a,b)} \tag{13}$$

Define $\{\omega_l\}_{l=0}^{\infty}$ s.t. $\omega_0 > 0$ and $\omega_{l+1} > \omega_l$ as frequency divisions. Let $F_l$ be the set of points $\omega' \in C$ closer to $\omega_l$ than any other $\omega_{l'}$ in the frequency bin. The SST of *f(t)* is defined as [5]

$$T_f(\omega_l, b) = \int_{\{a:\omega_f(a,b)\in F_l\}} W_f(a,b)a^{-3/2}da \tag{14}$$

### 3.3 Time-frequency analysis of non-stationary signals

To understand the intricacies of non-stationary signals, it is pivotal to delve into their time-frequency analysis. This section sets out to demonstrate the application of the Synchrosqueezing Transform (SST) method in such a context. For this purpose, a non-stationary signal is employed as an example.

$$x(t) = \cos\left(2\pi * (0.1t^{2.6} + 3\sin(2t) + 10t)\right) + e^{-0.2t}\cos\left(2\pi * (40 + t^{1.3})t\right) \tag{15}$$

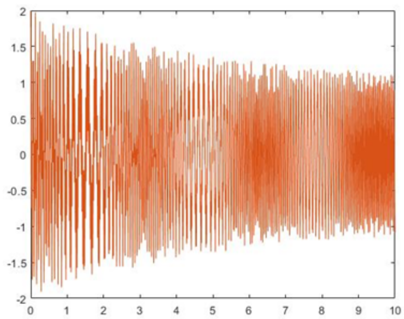


Figure 2. The non-stationary signal

Figure 2 shows the non-stationary signal. As shown in Equation (15), this signal consists of two components with time-varying frequencies: one introducing frequency drift and oscillations, and the other contributing amplitude decay, frequency drift, and variation. SST is used to obtain the time-frequency representation of this non-stationary signal and compared with that by STFT and CWT directly.

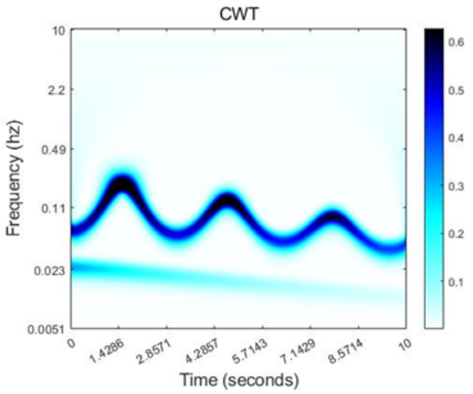


Figure 3. CWT of the signal

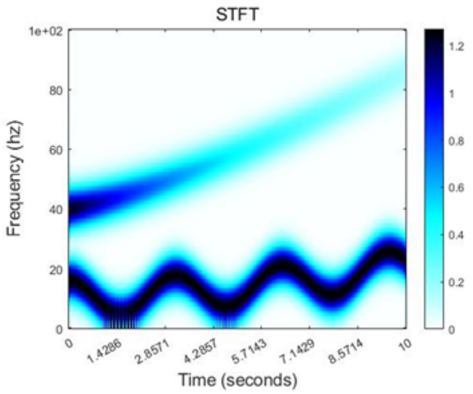


Figure 4. STFT of the signal

Figures 3 and 4 show the corresponding time-frequency representation using CWT and STFT respectively. In Figures 3 and 4, there are two clear signal components that are corresponding to two components in Equation (15). From the figures, the readability is low for these two components. This is due to the spectral smoothing and leakage. Especially for that by STFT, the resolution of the time-frequency representation is much low.

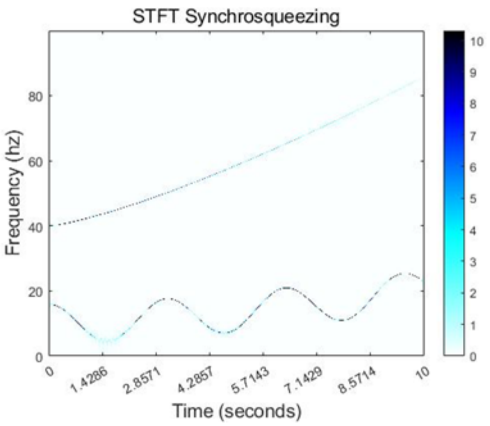


Figure 5. STFT based SST of the signal

Figures 5 and 6 show the time-frequency representation using the STFT and CWT based SST respectively. Compared with Figures 3 and 4, the time-frequency representations by SST algorithms have a high resolution with a high energy concentration. Their readability is also improved.

In a comparison of SST, STFT, and CWT methods for non-stationary signals, SST outperforms with a more concentrated and sharper time-frequency representation (TFR). Unlike STFT and CWT, which grapple with the time-frequency resolution trade-off, SST accurately depicts time-varying characteristics. This energy concentration in TFR aids in discriminating signal components and extracting precise features, offering a detailed understanding of signal dynamics.

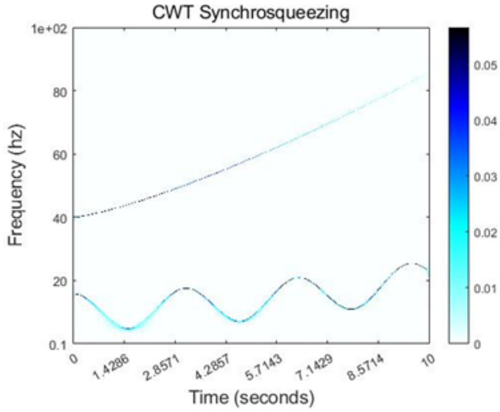


Figure 6. CWT based SST of the signal

### 3.4 *Time-varying characteristics of the VBI system with SST*

As discussed above, the SST method has a high readability for time-frequency analysis of non-stationary signals. The vehicle-bridge interaction (VBI) system is a time-varying system. In this study, the SST method will be used to extract the time-varying characteristics of the VBI system for bridge SHM. The VBI model is built firstly. The bridge with different damage scenarios is simulated. Then the STFT and CWT based SST algorithms are used to extract the time-varying characteristics from the bridge responses. The effect of different parameters on the time-varying characteristics will be studied in the next section.

## 4 EXPERIMENTAL STUDY

### 4.1 *Experimental Setup*

To verify the proposed method, an experimental study has been conducted in the laboratory. Figure 7 shows the vehicle-bridge interaction model in the laboratory. The bridge model includes three Tee-section concrete beams, i.e., the leading beam, the main beam and the tailing beam. The length of the leading and tailing beams are 4.5 m each. The main beam is for the testing bridge with a length of 5 m. The gaps between these beams are 10mm. A vehicle is pulled along the beam by an electric motor at an approximate speed of 0.5 m/s. The axle and wheel spacings of the vehicle are 0.8 m and 0.39 m respectively. The weight of the vehicle is 10.60kN with the front axle load of 5.58 kg and the rear axle load of 5.02 kg. The reinforced concrete beam with the large damage scenario is used in this study and the damage is created by adding 26kN at 1/3 and 2/3 span. The detail information can be found in the reference [2]. Seven accelerometers are installed evenly along the longitudinal direction of the beam. The acceleration response at the 3/8 span of the beam is used for time-varying analysis. The sampling frequency is 2024.292Hz.

In comparison, STFT is used to obtain the TFR as shown in Figure 8. Figure 9 shows the TFR of the response using the proposed SST method. From the figures, there is a clear frequency component around 11Hz. That is corresponding to the first natural frequency of the beam [2]. There is another component around 5Hz and that may be due to the vehicle-bridge interaction. Compared the TFR by the proposed SST method with that by STFT, the instantaneous frequency trajectory by SST is much clearer with a high energy concentration than that by STFT. That means the time-varying characteristics of the VBI by the proposed SST method has a high readability than that by STFT directly. The proposed SST method could effectively extract the instantaneous frequency from non-stationary signals without mode mixing problems, providing a more accurate original signal decomposition and superior time-frequency resolution.

Figure 7. The experimental VBI system

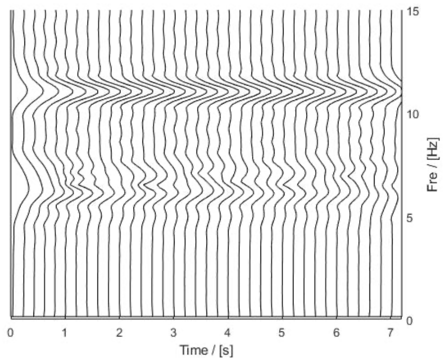


Figure 8. TFR of the response using STFT

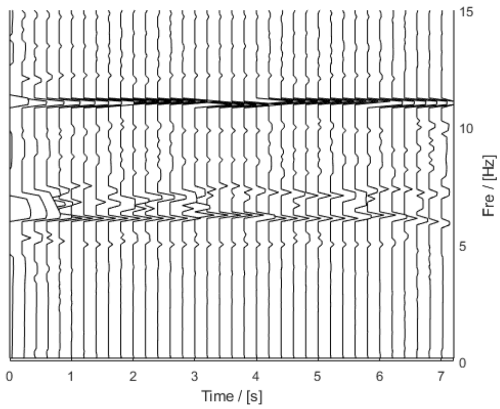


Figure 9. TFR of the response using SST

# 5 NUMERICAL STUDY

## *5.1 Parameters of the vehicle-bridge interaction model*

To further investigate the performance of the proposed SST method, the parametric study has been conducted in this section. The bridge model is same as that in the experimental study in Section 4. The length of the Tee-section beam bridge is 5 m. The first seven modes have been considered to construct the mass, damping, and stiffness matrices of the bridge model. The first natural frequency of the beam is 11.00Hz. The Rayleigh damping $C_b = \alpha_1 M_b + \alpha_2 K_b$ is used and $\alpha 1$ is 0.243 and $\alpha 2$ is 0.0001. The parameters of the vehicle are: $M_v$=1081kg, $K_v$=6.22e6 N/m, $C_v$=178N/m/s. The surface of the bridge deck is ignored in this study. It is postulated that the vehicle traverses a 5 m approach road before entering the bridge. The bridge-vehicle response is obtained by resolving the coupled vehicle-bridge interaction equation utilizing the Newmark-β method. A 500 Hz sampling rate is chosen based on the Nyquist sampling theorem to accurately capture the dynamic responses of the system.

## *5.2 Time-Frequency Analysis of Bridge Responses*

In this study, the proposed SST is used for time-frequency analysis of the VBI system. The passage of the vehicle over the bridge is time-varying process. Time-frequency spectra depicts the response patterns of the VBI system, showcasing energy distribution over time and frequency. A healthy bridge follows expected spectral patterns, while structural damage results in deviations such as frequency shifts or unusual energy distributions.

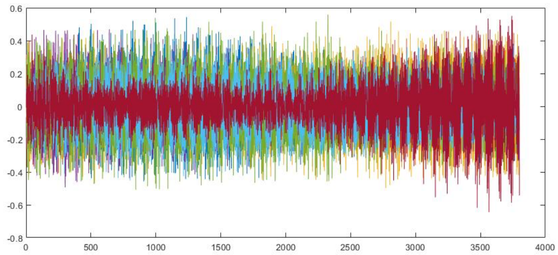


Figure 10. Acceleration of vehicle-bridge system

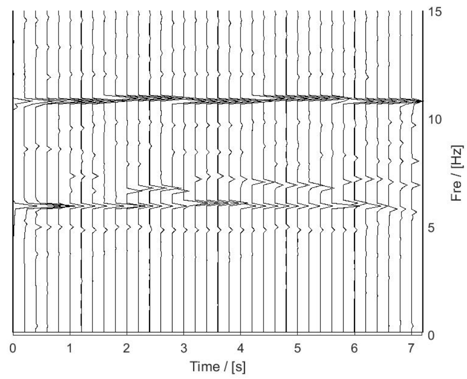


Figure 11. TFR of bridge response

Figure10 shows the acceleration responses of the bridge subject to the moving vehicle. Figure 11 shows the TFR by the proposed SST. From Figure 11, there are two clear components. The component around 11 Hz is corresponding to the natural frequency of the beam.

### 5.3 *Effect of different damage severities*

This section is to study the effect of the damage severity. The damage is summated by Equation (4). As shown in Equation (4), a damage zone is determined by a decay factor $\alpha$ and a regulation factor $\beta$ in the flexural rigidity $EI$ of the beam. The damage location is defined by the center position $Lc$ of the damage zone, and the range of the damage zone is determined by $\beta$.

Figure 11 shows the TFR for the bridge without the damage. In Figure 11, the TFR of the bridge response depicts a clear, unimpeded frequency pattern. This frequency pattern could be interpreted as the structural 'signature' or 'fingerprint' of the bridge, providing insight into its operational characteristics and status under nominal or undamaged conditions. This 'signature' can serve as a benchmark for assessing the bridge's structural health or integrity over time or under different loading conditions. Figure 12 shows the TFR of the bridge response for the bridge with the damage scenario $\alpha = 0.5$. Compared with Figure 11, the TFR of the bridge response exhibits a remarkable alteration in Figure 12. The frequency pattern, which was previously distinct and unambiguous, becomes notably obscured and blurred in the time-frequency domain. This could be attributed to the damage-induced changes in the bridge's structural characteristics, leading to alterations in its dynamic response. This phenomenon implies a significant reduction in the bridge's structural health and potentially its operational capacity.

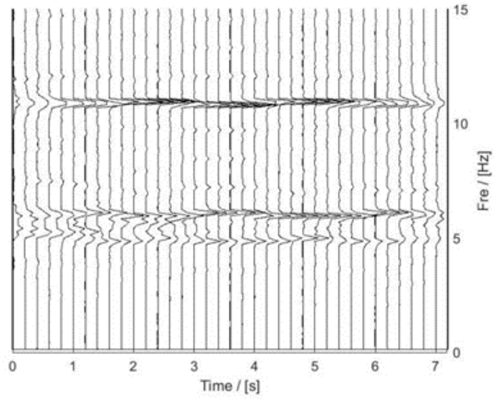


Figure 12. TFR with $\alpha = 0.5$

### 5.4 *Effect of different damage locations*

The effect of the damage location is studied in this section. Two damage scenarios are simulated with the centre of the damage zone at 1/2 and 1/3 span of the beam respectively.

Figures 13 and 14 show the TFR of the bridge responses with the damage at 1/2 and 1/3 span of the beam. There are instantaneous frequency trajectories around 11 Hz in these two figures. The instantaneous frequency is lower in Figure 13 than that in Figure 14. The results show that the damage at the middle span may have a more pronounced effect on the structure's behavior and could potentially lead to more significant changes in the TFR of the bridge response. In contrast, damage in areas of low stress may not drastically influence the TFR. Therefore, the location of damage significantly affects the overall performance and safety of the bridge structure.

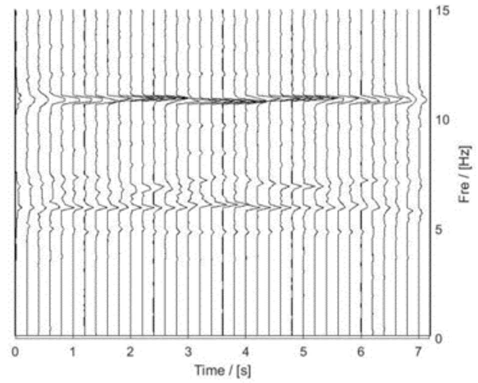


Figure 13. TFR with the damage at 1/2 span

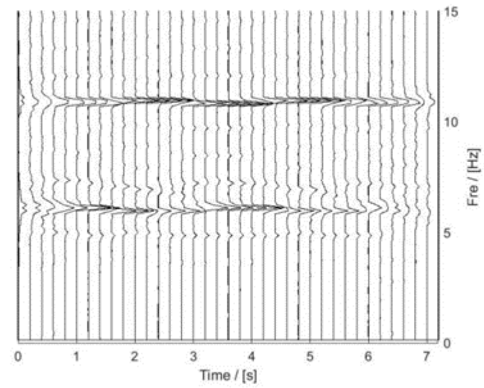


Figure 14. TFR with the damage at 1/3 span

## 6 CONCLUSIONS

A synchrosqueezing transform (SST) based method has been developed to extract the time-varying characteristics of the vehicle-bridge interaction (VBI) system for bridge structural health monitoring. Numerical and experimental results have shown that the time-varying characteristics of the VBI system by the proposed method could be a potential indicator of the damage in the bridge. Further study is needed for applications in practice.

## REFERENCES

[1] X.Q. Zhu and S.S. Law. Structural health monitoring based on vehicle-bridge interaction: accomplishments and challenges. *Advances in Structural Engineering*, 18(12), 1999-2015, 2015.

[2] S.S. Law and X.Q. Zhu. Nonlinear characteristics of damaged concrete structures under vehicular loads. *Journal of Structural Engineering ASCE*, 131(8), 1277-1285, 2005.

[3] J.B. Tary, R.H. Herrera and M. van der Baan. Analysis of time-varying signals using continuous wavelet and synchrosqueezed transform. *Philosophical Transactions A: Mathematical, Physical and Engineering Sciences*, 376, 20170254, 2018.

[4] L. Li, H.Y. Cai, H.X. Han, Q.T. Jiang and H.B. Ji. Adaptive short-time Fourier transform and synchrosqueezing transform for non-stationary signal separation. *Signal Processing*, 166, 107231, 2020.

[5] Q.T. Jiang and B.W. Suter. Instantaneous frequency estimation based on synchrosqueezing wavelet transform. *Signal Processing*, 138, 167-181, 2017.
[6] J.T. Li, X.Q. Zhu, S.S. Law and B. Samali. Time-varying characteristics of bridges under passage of vehicles using synchroextracting transform. *Mechanical Systems and Signal Processing*, 140, 206727, 2020.
[7] J. Zhang, D. Yang, W.X. Ren and Y. Yuan. Time-varying characteristics analysis of vehicle-bridge interaction system based on modified S-transform reassignment technique. *Mechanical Systems and Signal Processing*, 160, 107807, 2021.
[8] C.J. Tan, H. Zhao, E.J. Obrien, N. Uddin and C.-W. Kim. Exploring time-varying characteristics in drive-by bridge frequency extraction with the second-order synchrosqueezing transform. *Journal of Bridge Engineering ASCE*, 28(4), 040230, 2023.
[9] S.S. Law and X.Q. Zhu. Dynamic behavior of damaged concrete bridge structures under moving vehicular loads. *Engineering Structures*, 26, 1279-1293, 2004.